THE JOURNAL OF BIOLOGICAL CHEMISTRY VOL. 283, NO. 40, pp. 27038–27047, October 3, 2008

Phosphorylation of Endothelial Nitric-oxide Synthase Regulates Superoxide Generation from the Enzyme*

Received for publication, March 21, 2008, and in revised form, July 1, 2008 Published, JBC Papers in Press, July 13, 2008, DOI 10.1074/jbc.M802269200

Chun-An Chen, Lawrence J. Druhan, Saradhadevi Varadharaj, Yeong-Renn Chen, and Jay L. Zweier[1]

From the Davis Heart and Lung Research Institute and The Division of Cardiovascular Medicine, Department of Internal Medicine, The Ohio State University College of Medicine, Columbus, Ohio 43210

In the vasculature, nitric oxide (NO) is generated by endothelial NO synthase (eNOS) in a calcium/calmodulin-dependent reaction. With oxidative stress, the critical cofactor BH_4 is depleted, and NADPH oxidation is uncoupled from NO generation, leading to production of (O_2^-). Although phosphorylation of eNOS regulates *in vivo* NO generation, the effects of phosphorylation on eNOS coupling and O_2^- generation are unknown. Therefore, we phosphorylated recombinant BH_4-free eNOS *in vitro* using native kinases and determined O_2^- generation using EPR spin trapping. Phosphorylation of Ser-1177 by Akt led to an increase (>50%) in maximal O_2^- generation from eNOS. Moreover, Ser-1177 phosphorylation greatly altered the Ca^{2+} sensitivity of eNOS, such that O_2^- generation became largely Ca^{2+}-independent. In contrast, phosphorylation of eNOS at Thr-495 by protein kinase Cα (PKCα) had no effect on maximum activity or calcium sensitivity but decreased calmodulin binding and increased association with caveolin. In endothelial cells, eNOS-dependent O_2^- generation was stimulated by vascular endothelial growth factor that induced phosphorylation of Ser-1177. With PKC activation that led to phosphorylation of Thr-495, no inhibition of O_2^- generation occurred. As such, phosphorylation of eNOS at Ser-1177 is pivotal in the direct regulation of O_2^- and NO generation, altering both the Ca^{2+} sensitivity of the enzyme and rate of product formation, whereas phosphorylation of Thr-495 indirectly affects this process through regulation of the calmodulin and caveolin interaction. Thus, Akt-mediated phosphorylation modulates eNOS uncoupling and greatly increases O_2^- generation from the enzyme at low Ca^{2+} concentrations, and PKCα-mediated phosphorylation alters the sensitivity of the enzyme to other negative regulatory signals.

Nitric-oxide synthase (NOS)[2] is a critical enzyme that converts L-arginine (L-Arg) to L-citrulline and nitric oxide (NO) with the consumption of NADPH. NO is a signaling molecule that promotes vascular smooth muscle relaxation and functions as an endogenous mediator of a wide range of effects in different tissues (1, 2). After oxidant stress, as occurs in post-ischemic tissues, production of O_2^- and its derived oxidants, including peroxynitrite ($ONOO^-$), hydrogen peroxide (H_2O_2), and hydroxyl radical (·OH), induce NOS dysfunction with uncoupling of the enzyme leading to the production of NOS-derived O_2^- instead of NO (3, 4). It has been reported that an imbalance between NO and O_2^- can contribute to the onset of a variety of cardiovascular diseases, including hypertension, atherosclerosis, and heart failure (5). Therefore, tight coupling of the enzyme is important for normal cardiovascular function and prevention of disease.

The catalytic domains of NOS include a flavin-containing NADPH binding reductase and a heme-binding oxygenase that also contains the binding sites for the redox labile cofactor tetrahydrobiopterin (BH_4) and the substrate L-Arg. In the presence of Ca^{2+} and calmodulin (CaM), electrons flow from NADPH through the reductase domain to the oxygenase domain resulting in the activation of oxygen at the heme center followed by substrate monooxygenation. This process requires the presence of the fully reduced BH_4. Our laboratory and several others have demonstrated that besides synthesizing NO, all three isoforms of NOS can also generate O_2^-, depending on substrate and cofactor availability (3, 6–9). One of the primary mechanisms implicated in the oxidant-induced switch of NOS from the production of NO to the generation of O_2^- is the oxidation of the enzyme bound BH_4 (10, 11).

Various extracellular signals, including shear stress and additional stimuli such as vascular endothelial growth factor (VEGF), estrogen, sphingosine 1-phosphate, bradykinin, and aldosterone, modulate eNOS NO generation through several signal transduction pathways (12–16). Cellular studies have demonstrated that phosphorylation of eNOS at specific amino acids regulates enzyme-mediated NO production (17). The majority of previous work has focused on two residues, serine 1177 and threonine 495. It has been shown that Akt specifically induces phosphorylation of Ser-1177 (18, 19) and that PKC specifically phosphorylates Thr-495 (20). Although phosphorylation of Ser-1177 has been shown to increase NO production

* This work was supported, in whole or in part, by National Institutes of Health Grants HL63744, HL65608, and HL38324 (to J. L. Z.) and HL83237 (Y.-R. C.). This work was also supported by an American Heart Association postdoctoral fellowship (to C.-A. C.). The costs of publication of this article were defrayed in part by the payment of page charges. This article must therefore be hereby marked "*advertisement*" in accordance with 18 U.S.C. Section 1734 solely to indicate this fact.

[1] To whom correspondence should be addressed: Davis Heart and Lung Research Institute, 473 W. 12th Ave., Columbus, OH 43210. Tel.: 614-247-7857; Fax: 614-247-7845; E-mail: Jay.Zweier@osumc.edu.

[2] The abbreviations used are: NOS, nitric-oxide synthase; eNOS, endothelial NOS; heNOS, human eNOS; beNOS, bovine eNOS; PKC, protein kinase C; BAECs, bovine aortic endothelial cells; CaI, calcium ionophore; CaM, calmodulin; Cav-P, caveolin peptide; DAPI, 4′,6-diamidino-2-phenylindole dihydrochloride; DEPMPO, 5-diethoxyphosphoryl-5-methyl-1-pyrroline *N*-oxide; DHE, dihydroethidine; DTT, dithiothreitol; EPR, electron paramagnetic resonance; HE, hydroethidine; L-NAME, L-N^G-nitroarginine methyl ester hydrochloride; BH_4, tetrahydrobiopterin; TBST, Tris-buffered saline (TBS) and Tween; VEGF, vascular endothelial growth factor; RT, room temperature; PMA, phorbol 12-myristate 13-acetate.

from eNOS (21), in contrast, phosphorylation of Thr-495 has been reported to down-regulate NO generation (18, 22, 23).

Although there is strong evidence indicating that phosphorylation of eNOS is involved in directly modulating eNOS-mediated NO generation, the definitive mechanisms involved remain unclear. Moreover, there is a lack of prior investigation directed toward understanding how phosphorylation alters O_2^- generation from the uncoupled enzyme. Determination of the effects of phosphorylation on eNOS-derived O_2^- generation is of particular importance, because of the implications of this regulation in cardiovascular disease and other physiological settings in which eNOS is uncoupled (3, 4). Delineation of the mechanisms involved in the phosphorylation-dependent regulation of uncoupled eNOS will provide critical insights regarding the pathophysiology of eNOS dysfunction.

Therefore, studies were performed to investigate how phosphorylation by the critical signaling kinases Akt or PKCα modulates eNOS uncoupling and the production of O_2^- from the enzyme. Studies were performed with *in vitro* phosphorylation of recombinant human eNOS and also with intact endothelial cells. Our results demonstrated that phosphorylation of eNOS at Ser-1177 is pivotal in the regulation of O_2^- generation, altering both the Ca^{2+} sensitivity of the enzyme and maximal rate of product generation, whereas phosphorylation of Thr-495 indirectly affects O_2^- generation by modulating the binding of proteins known to regulate the activity of the enzyme.

EXPERIMENTAL PROCEDURES

Materials—Akt1 kinase, PKCα kinase, anti-eNOS antibody, anti-phospho-Ser-1177, and anti-phospho-Thr-495 eNOS antibodies were purchased from Cell Signaling Technology, Inc. (Danvers, MA). Terrific broth, LB broth base, EZQ phosphoprotein quantification kit, dithiothreitol (DTT), and carbenicillin were obtained from Invitrogen. Protease inhibitor mixture tablets were purchased from Roche. NADPH, L-Arg, and hemoglobin were purchased from Sigma-Aldrich. Isopropyl β-D-1-thiogalactopyranoside was purchased from Anatrace, Inc. (Maumee, OH). Chloramphenicol was obtained from Fluka (St. Louis, MO). 5-Diethoxyphosphoryl-5-methyl-1-pyrroline *N*-oxide (DEPMPO) was purchased from Alexis Biochemicals (San Diego, CA). Caveolin peptide (Cav-P) was custom-synthesized by Bio-Synthesis Inc. (Lewisville, TX). The sequence of Cav-P is DGIWKASFTTFTVTKYWFYR (24).

Protein Expression and Purification—The bacterial expression plasmid of pCWheNOS was a gift from Dr. Ortiz de Montellano from University of California at San Franscisco. Overexpression of active human eNOS in *Escherichia coli* was greatly enhanced by coexpression with calmodulin (pCaM). Typically, a 10-ml LB overnight culture of pCWheNOS and pCaM in BL21(DE3) *E. coli* was used to inoculate 1 liter of terrific broth in a 4-liter flask containing 125 μg/ml carbenicillin and 50 μg/ml chloramphenicol. The culture was grown at 37 °C until the cell density reached an A_{600} of 0.8, then δ-aminolevulinic acid was added to a final concentration of 0.5 mM, and the cells were induced by the addition of isopropyl β-D-1-thiogalactopyranoside (1 mM final concentration). The cultures were then grown at 22 °C at 200 rpm for 20 h before harvest by centrifugation at 4 °C. The cell pellet was stored at −80 °C until purification (25, 26).

Typically, 2 liters of human eNOS (heNOS)-expressing cells were pelleted and resuspended in 50 ml of lysis buffer containing 40 mM HEPES, pH 7.6, 10% glycerol, 500 mM NaCl, 40 mM imidazole, 1 mM DTT, 10 μM BH_4, and 5 tablets of protease inhibitor mixture, EDTA free. The cells were lysed in the presence of 20 mg/ml lysozyme on ice for 30 min with stirring by pulse sonication 10 s each cycle with a total of ~15 cycles. During the sonication the solution was always kept below 4 °C to prevent any degradation or inactivation of the enzyme. The cell debris was cleared by centrifugation at 48,000 × *g* for 1 h at 4 °C. The supernatant was applied to a 5-ml HisTrap nickel-nitrilotriacetic acid column (GE Healthcare) equilibrated with lysis buffer using an AKTA fast protein liquid chromatography system (GE Healthcare). The column was then washed with 10 column volumes of buffer A (40 mM HEPES, pH 7.6, 10% glycerol, 40 mM imidazole, 1 mM DTT, 10 μM BH_4). Finally the heNOS was eluted with buffer B (40 mM HEPES, pH 7.6, 10% glycerol, 500 mM NaCl, 250 mM imidazole, 1 mM DTT, 10 μM BH_4). The colored fractions were pooled, and 20 mM L-Arg, 20 μM BH_4, and 5 mM DTT were added and incubated on ice for 4 h. The purified protein was subsequently loaded into Hi-Load Superdex 200 size exclusion column equilibrated with buffer C (40 mM HEPES, pH 7.6, 10% glycerol, 150 mM NaCl, 1 mM DTT). The colored fractions were pooled and concentrated to greater than 1 mg/ml by ultrafiltration. The concentrated protein was separated into aliquots and quickly frozen in liquid nitrogen before storage at −80 °C. When heNOS was coexpressed with CaM, 2 mM $CaCl_2$ was included in all purification buffers (26). Because of the instability of purified heNOS, the entire purification process was completed within 1 day. For the BH_4-free heNOS, used for O_2^- determinations, L-Arg and BH_4 were excluded during the purification process. To remove CaM from the heNOS purification, 2 mM EGTA was included in Buffer C.

Phosphorylation of heNOS by Akt and PKCα—heNOS (5 μM, 0.675 μg/μl) was phosphorylated at RT for 20 min with Akt or PKCα (100 ng) in a total volume of 20 μl in 1× kinase buffer containing 25 mM Tris-HCl, pH 7.5, 10 mM $MgCl_2$, 5 mM β-glycerophosphate, 0.1 mM Na_3VO_4, 2 mM DTT, 200 μM ATP according to manufacturer's protocol. After phosphorylation, the phosphorylated heNOS was subjected to immunoblotting analysis or EZQ phosphoprotein determination. The Invitrogen EZQ phosphoprotein quantification kit was used to determine the phosphorylation efficiency of heNOS by Akt and PKCα. According to the procedures in the manufacture's manual, the phosphorylated heNOS by Akt, PKCα, or both was spotted onto specially prepared assay paper, fixed onto the paper with methanol, and then stained with EZQ phosphoprotein quantification reagent. The dried assay paper was inserted onto EZQ 96-well microplate cassette, and the stained protein spots were analyzed in a fluorescence-based reader (SpectraMax GEMINIXS, Molecular Devices, Sunnyvale, CA) using excitation/emission wavelengths of 550/580 nm. Relative phosphate content of phosphorylated heNOS was determined from a standard curve of ovalbumin, which contains two phosphate groups per molecule. The control experiments with kinase alone were always performed, and the fluorescent intensity of control experiments was subtracted from all experiments.

Protein and Heme Content Determination—Protein concentration of purified heNOS was determined by the Bradford assay from Bio-Rad using a bovine serum albumin standard. The heme content of the purified heNOS was determined by pyridine hemochromogen assay. 50 μg of heNOS was added to a solution containing 0.15 M NaOH and 1.8 M pyridine, and the difference spectrum (reduced minus oxidized bispyridine heme) was recorded using $\Delta\epsilon = 24\ mM^{-1}\ cm^{-1}$ at 556–538 nm (27). The reduced bispyridine heme was generated by the addition of a few grains of dithionite.

SDS-PAGE and Immunoblotting—The reaction mixture was mixed with the sample loading buffer at a ratio 3:1 (v/v), incubated at 80 °C for 10 min, and then immediately loaded onto a 4–20% Tris-glycine polyacrylamide gradient gel. Samples were run at room temperature for 1.5 h at 125 V. Protein bands were electrophoretically transferred to a nitrocellulose membrane in 12 mM Tris, 96 mM glycine, and 20% methanol with a Xcell II Blot Module from Invitrogen with 25 V constant for 90 min. Membranes were blocked for 1 h at room temperature in Tris-buffered saline (TBS) containing 0.05% Tween 20 (TBST) with 5% dry milk (Bio-Rad). Membranes were then incubated overnight with anti-eNOS, anti-phospho-Thr-495, or anti-phospho-Ser-1177 eNOS polyclonal antibodies at 4 °C. Membranes were then washed 3 times in TBST and incubated for 1 h with horseradish peroxidase-conjugated anti-rabbit IgG in TBST at room temperature. Membranes were again washed three times in TBST and then visualized using ECL immunoblotting detection reagents (Amersham Biosciences). The signal intensity of blotting was digitized and quantified using an AlphaImager™ high performance gel documentation and image analysis system, model 3300 (Alpha Innotech Co. San Leandro, CA).

Measurement of O_2^- Generation by EPR Spin Trapping—Spin-trapping measurements of oxygen radicals were performed in 50 mM Tris-HCl buffer, pH 7.4, containing 0.5 mM NADPH, 0.5 mM Ca^{2+}, 10 μg/ml CaM, 15 μg/ml purified heNOS, and 25 mM spin trap DEPMPO. EPR spectra were recorded in a 50-μl capillary at room temperature with a Bruker EMX spectrometer operating at 9.86 GHz with 100 kHz modulation frequency as described (28, 29). The sample was scanned using the following parameters: center field, 3510 G; sweep width, 140 G; power, 20 milliwatts; receiver gain, 2×10^5; modulation amplitude, 1 G; time of conversion, 41 ms; time constant, 328 ms.

Ca^{2+} Dependence of O_2^- Generation from heNOS—100 μl of reaction volume was typically used for EPR measurements containing 100 μM EGTA. The reaction was initiated by the addition of 0.5 mM NADPH. The O_2^- measurements were performed by EPR spin-trapping as described above. The free Ca^{2+} concentration in the Ca^{2+} dependence studies was calculated using winmaxc32 program version 2.5 (Stanford University) (30, 31) accounting for pH and buffer components of phosphorylation reactions and 100 μM EGTA.

Cav-P Inhibition of O_2^- Generation from heNOS—A 100-μl reaction volume was typically used for EPR measurements, identical to that described above except that Cav-P (400 μM final concentration) was added to each reaction. The reaction was initiated by the addition of 0.5 mM NADPH. The O_2^- measurements were performed and quantified by EPR spin-trapping as described above.

Measurement of O_2^- from Uncoupled eNOS in Endothelial Cells—Bovine aortic endothelial cells (BAECs) cultured on sterile coverslips (Harvard Apparatus, 22 mm^2) in 35-mm sterile dishes at a density of 10^4 cells/dish were subjected to BH_4 depletion. To deplete BH_4, BAECs were treated with 5 mM 2,4-diamino-6-hydroxypyrimidine, an inhibitor of GTPCH1 (GTP-cyclohydrolase I) involved in BH_4 biosynthesis, for 18 h (32). For VEGF treatment (22), a final concentration of 50 ng/ml VEGF was added to BAECs or 2,4-diamino-6-hydroxypyrimidine-treated BAECs for 10 min to activate Ser-1179 phosphorylation of bovine eNOS (beNOS). Ionomycin (calcium ionophore (CaI)) (22) was added to a final concentration of 1 μM in control BAECs or BAECs with 2,4-diamino-6-hydroxypyrimidine treatment for 10 min. The phosphorylation of beNOS at Thr-497 was achieved by the addition of phorbol 12-myristate 13-acetate (PMA) to a final concentration of 0.1 μM for 10 min (22). For negative control experiments, L-N^G-nitroarginine methyl ester (L-NAME), a NOS inhibitor was added to a final concentration of 1 mM, 15 min before VEGF, PMA, or CaI treatments. Cells were then incubated with the O_2^- indicator 10 μM dihydroethidine (DHE) to detect O_2^- in live cells. DHE fluoresces when oxidized by O_2^-. Nuclei were stained with blue fluorescent DAPI (1 μM) for 10 min in the incubator. After the incubation, cells were washed with 1× phosphate-buffered saline and mounted using a mounting medium Fluoromount-G, and images were captured and analyzed at a magnification of 20× for DHE and DAPI by confocal fluorescence microscopy (LSM 510; Zeiss Inc., Peabody, MA) and overlaid using LSM software.

Immunofluorescence Microscopy—BAECs cultured on sterile coverslips (Harvard Apparatus, 22 mm^2) in 35-mm sterile dishes at a density of 10^4 cells/dish were subjected to BH_4 depletion and Ser-1179 and Thr-497 phosphorylation, as described in the previous section. At the end of the experiment, cells attached to coverslips were washed with 1× phosphate-buffered saline and fixed with 3.7% paraformaldehyde for 10 min, permeabilized with 0.25% Triton X-100 in TBST containing 0.01% Tween 20 for 5 min, and blocked for 30 min with 1% bovine serum albumin in 0.01% TBST. For visualization of beNOS Ser-1179 and Thr-497 phosphorylation, the fixed and permeabilized cells were incubated with rabbit primary anti-phospho-Ser-1179 and anti-phospho-Thr-497 eNOS antibodies, respectively, at a dilution of 1:2000 in 0.01% TBST containing 1% bovine serum albumin for 1 h at room temperature followed by an anti-rabbit AlexaFluor 488-conjugated antibody (1:1000 dilution) for 1 h at room temperature. The coverslips with cells were then mounted on a glass slide with the antifade mounting medium and viewed with a Zeiss confocal microscope at a magnification of 60×, and images were captured digitally.

RESULTS

Protein Expression, Purification, and Characterization—To mitigate problems with low yield and instability of heNOS when expressed in an *E. coli* system, recombinant human eNOS was coexpressed with CaM as reported previously (26) and iso-

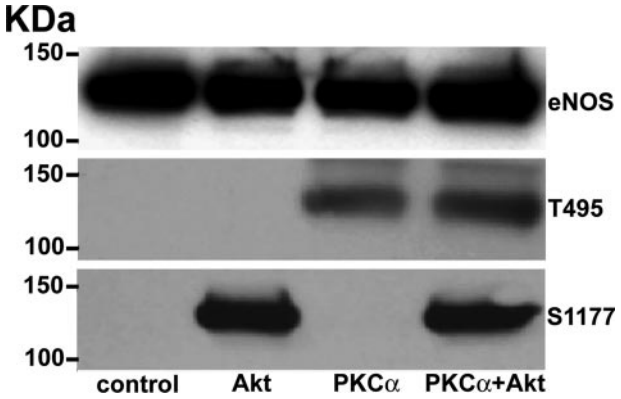

FIGURE 1. **Immunoblotting of phosphorylated heNOS at Thr-495 and Ser-1177.** *Upper panel*, a loading control, blotted against eNOS antibody. *Middle panel*, heNOS was phosphorylated *in vitro* by PKCα, Akt, or Akt and PKCα at RT for 20 min and blotted against anti-phospho-Thr-495 eNOS polyclonal antibody. *Lower panel*, heNOS was phosphorylated *in vitro* by PKCα, Akt, or Akt and PKCα at RT for 20 min and blotted against anti-phospho-Ser-1177 eNOS polyclonal antibody.

lated using nickel-nitrilotriacetic acid affinity and size exclusion chromatography. The coexpression of heNOS with CaM increased the yield 3-fold compared with expression of heNOS alone (3 mg/liter *versus* 1 mg/liter), consistent with previous reports (26). The purified protein preparations exhibited one prominent band (>95% pure) on 4–20% SDS-PAGE with Coomassie staining. The molecular weight of the purified protein, 135 kDa, is in accordance with the molecular mass for native heNOS monomer (3, 10, 33), and the identity of this band was confirmed by immunoblotting using an anti-eNOS antibody (Fig. 1), and mass spectrometry (data not shown). The NO generation, as determined by monitoring the conversion of oxyhemoglobin to ferric methemoglobin from the recombinant protein, was consistent with reported values (100–140 nmol·min^{-1}·mg^{-1}) (3, 26), and as expected the catalytic activity was dependent upon the addition of Ca^{2+} and CaM and could be totally blocked by the NOS inhibitor, L-NAME (1 mM).

Phosphorylation of heNOS by Akt and PKCα—Purified recombinant heNOS was phosphorylated at Ser-1177, Thr-495, or at both sites using the kinases Akt and PKCα in the presence of 1× kinase buffer at RT. The reactions reached completion by 20 min for both Akt and PKCα based on Akt phosphorylation time course immunoblotting. The phosphorylation events were confirmed by immunoblotting with anti-phospho-Ser-1177 and anti-phospho-Thr-495 antibodies (Fig. 1). These results indicated that Akt specifically phosphorylated heNOS at Ser-1177, whereas PKCα phosphorylation was specific for Thr-495. Additionally, equivalent phosphorylation of both sites occurs when using both Akt and PKCα. The extent of phosphorylation of heNOS at each site was determined by EZQ phosphoprotein quantitation kit. The phosphorylation of heNOS at Ser-1177 by Akt was determined to be ~80%, and the phosphorylation of Thr-495 by PKCα was determined to be close to 100% (34).

Effect of Phosphorylation of heNOS by Akt and PKCα on Its O_2^- Generation—Under certain conditions NOS-dependent NADPH oxidation is uncoupled from NO generation. This uncoupling occurs when either the substrate L-Arg or the redox active cofactor BH_4 is not present. EPR spin-trapping was used to directly measure the magnitude of O_2^- generation from

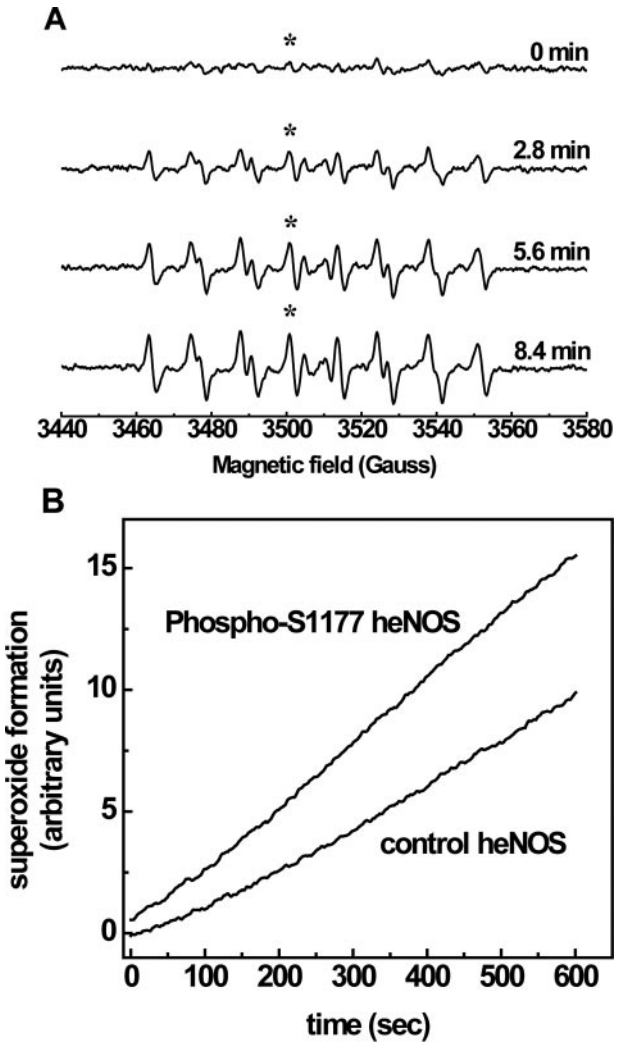

FIGURE 2. **EPR spin-trapping of the kinetics of O_2^- generation from control heNOS and phospho-Ser-1177 heNOS.** *A*, incremental scanning EPR spectra of oxygen free radical generation. The reaction system contains 50 mM Tris-HCl buffer, pH 7.4, 0.5 mM NADPH, 0.5 mM Ca^{2+}, 10 μg/ml CaM, 15 μg/ml purified heNOS, and 25 mM spin trap DEPMPO. Spectra were recorded at room temperature with a microwave frequency of 9.863 GHz, 20 milliwatts of microwave power, and 1.0 G modulation amplitude. Center field was 3510 G with 140-G sweep width. Time constant was 328 ms; each spectrum was an 84-s acquisition. *B*, the continuous time course of O_2^- generation from control and phospho-Ser-1177 heNOS was measured by fixing the static field at 3501.1 G on the maximum of the 4th peak of the DEPMPO-OOH adduct, as marked by the asterisk. The time constant was 5243 ms. The reaction system and acquisition parameters were otherwise the same as in *A*.

heNOS. Purified BH_4-free heNOS (5 μg) was incubated with 1× kinase buffer in the presence or absence of any kinase in a volume of 10 μl at RT for 20 min before DEPMPO spin-trapping. For the measurement of O_2^- production, this 10-μl reaction mixture was diluted into a total volume of 100 μl containing only Ca^{2+}/CaM, and the reaction was initiated by the addition of NADPH to a final concentration of 0.5 mM. EPR measurements were carried out, as described under "Experimental Procedures," with the nitrone spin trap DEPMPO, which forms a stable O_2^- adduct with a half-life of ~16 min (28). Kinetics of O_2^- generation from heNOS were determined by setting the static field at ~3501.1 G, on the maximum of the fourth peak of the EPR spectrum of the DEPMPO/·OOH spin trap adduct (Fig. 2*A*). The reaction rate of O_2^- generation was

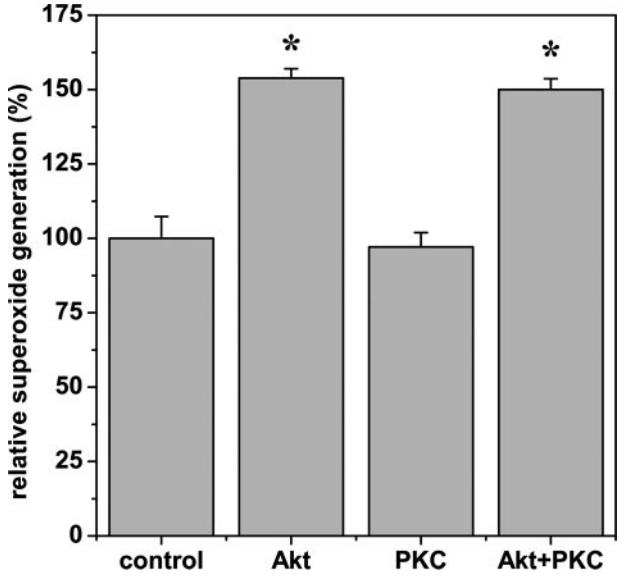

FIGURE 3. **Effects of phosphorylation on the magnitude of $O_2^{\cdot-}$ generation from heNOS.** $O_2^{\cdot-}$ generation rates from control and phosphorylated heNOS were determined from preparations of enzyme by EPR spin-trapping with DEPMPO as described in Fig. 2. The phosphorylation of heNOS by Akt or Akt and PKCα increased its $O_2^{\cdot-}$ generation by greater than 50%; however, there was no significant effect from the phosphorylation of heNOS by PKCα. Data were expressed as the mean ± S.E., $n = 3$ (*, $p < 0.001$ *versus* control).

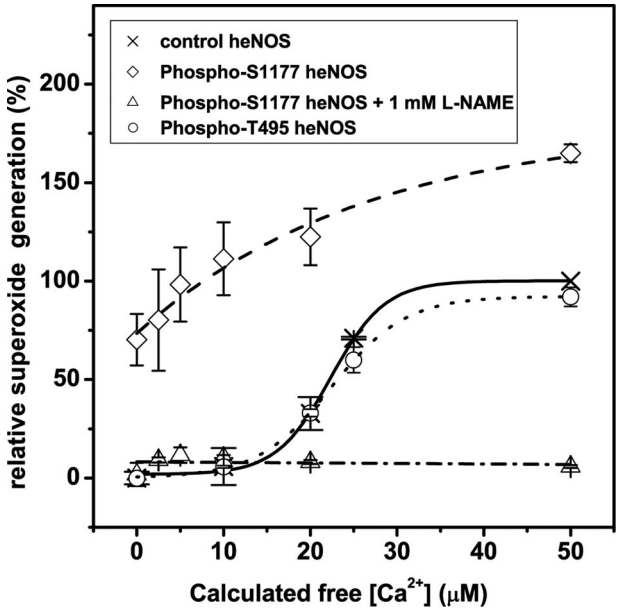

FIGURE 4. **Ca^{2+} dependence of $O_2^{\cdot-}$ generation from control, phospho-Ser-1177, and phospho-Thr-495 heNOS.** $O_2^{\cdot-}$ generation rates from control, phospho-Ser-1177, and phospho-Thr-495 heNOS were determined by EPR spin-trapping with DEPMPO as described in Fig. 2. In the reaction 100 μM EGTA was included in the assay buffer. The desired Ca^{2+} concentration was achieved by the addition of a concentrated $CaCl_2$ stock solution. The free [Ca^{2+}] was calculated as described under "Experimental Procedures." $O_2^{\cdot-}$ generation from eNOS was almost totally blocked by 1 mM L-NAME over the full range of Ca^{2+} concentrations studied. All data points show the relative magnitude of $O_2^{\cdot-}$ generation compared with the maximal values measured from control heNOS and correspond to the mean ± S.E. from triplicate experiments.

determined by a linear fitting of this signal amplitude change *versus* time during the first 5 min of reaction (Fig. 2*B*). The relative activities were further calculated by comparison with control experiments of unmodified heNOS.

Compared with the control enzyme, phosphorylation of heNOS at Ser-1177 increased $O_2^{\cdot-}$ generation by 54% ± 3% (Fig. 3). However, there was no significant effect on $O_2^{\cdot-}$ generation produced by phosphorylation of Thr-495. Furthermore, phosphorylation of heNOS by both Akt and PKCα increased its $O_2^{\cdot-}$ generation by a similar magnitude, 50% ± 4%, as seen with phosphorylation by Akt alone.

Ca^{2+} Dependence of Phosphorylation of heNOS on $O_2^{\cdot-}$ Generation—The generation of $O_2^{\cdot-}$ from eNOS is regulated by Ca^{2+}/CaM, and as noted above, phosphorylation of heNOS at Ser-1177 caused a marked increase in $O_2^{\cdot-}$ production. Therefore, studies were performed to examine how phosphorylation of this residue alters the Ca^{2+} sensitivity of the uncoupled BH_4-free enzyme. The desired free Ca^{2+} concentration was achieved by including 100 μM EGTA in the reaction mixture, with subsequent addition of $CaCl_2$ stock solution. The free Ca^{2+} concentration was then calculated as described under "Experimental Procedures." Plotting free [Ca^{2+}] *versus* activity and fitting the data with the Hill equation, we found that phosphorylation at Ser-1177 decreased the EC_{50} of Ca^{2+} for $O_2^{\cdot-}$ generation to a much lower concentration, 4.5 μM for the phospho-Ser-1177 eNOS compared with 22.1 μM for native eNOS (Fig. 4; Table 1). Thus, phosphorylation of heNOS at Ser-1177 triggered $O_2^{\cdot-}$ generation at much lower Ca^{2+} concentrations compared with non-phosphorylated heNOS, demonstrating ~45% of maximal $O_2^{\cdot-}$ generation even in the absence of free Ca^{2+}. The NOS inhibitor L-NAME, which is known to inhibit both NO and $O_2^{\cdot-}$ generation from eNOS, was able to almost totally block $O_2^{\cdot-}$ production from the phosphorylated enzyme over the full range of Ca^{2+} concentrations studied. PKCα phosphorylation, however, only slightly altered the Ca^{2+}-dependent activation of $O_2^{\cdot-}$ generation compared with that of non-phosphorylated heNOS (23.2 *versus* 22.1 μM) (Fig. 4; Table 1).

TABLE 1

Effects of heNOS phosphorylation on Ca^{2+}, CaM activation, or Cav-P inhibition of $O_2^{\cdot-}$ generation

$O_2^{\cdot-}$ generation rates from control and Akt or PKCα–phosphorylated heNOS (BH_4-free) were measured by EPR spin-trapping as described in Fig. 2 with EC_{50} measured as in Figs. 4 and 6. The effect of phosphorylation of heNOS on the interaction with Cav-P was determined with Cav-P inhibition expressed as the percent inhibition produced by the addition of Cav-P (400 μM) to a reaction containing 500 μM Ca^{2+}, 600 nM CaM.

	EC_{50} of [calcium]	EC_{50} of [CaM]	Cav-P inhibition of superoxide generation
	μM	nM	%
Control	22.1	208	35.7 ± 3.9
Akt	4.5	149	50.6 ± 2.6[a]
PKCα	23.2	496	67.8 ± 1.6[b]

[a] $p < 0.02$ *versus* control.
[b] $p < 0.01$ *versus* control. Data are expressed as the mean ± S.E., $n = 3$.

EGTA Inactivation of $O_2^{\cdot-}$ Generation from heNOS—In these experiments the active eNOS·CaM·Ca^{2+} complex was allowed to form, and then increasing concentrations of EGTA were added to chelate the Ca^{2+} and initiate the dissociation of the complex. After 1 min, the rate of $O_2^{\cdot-}$ generation was determined using EPR spin-trapping, as described above. At an EGTA concentration of 800 μM, no $O_2^{\cdot-}$ signal was detected from the non-phosphorylated enzyme; however, the phospho-Ser-1177 eNOS still retained ~40% of its maximal $O_2^{\cdot-}$ generation capac-

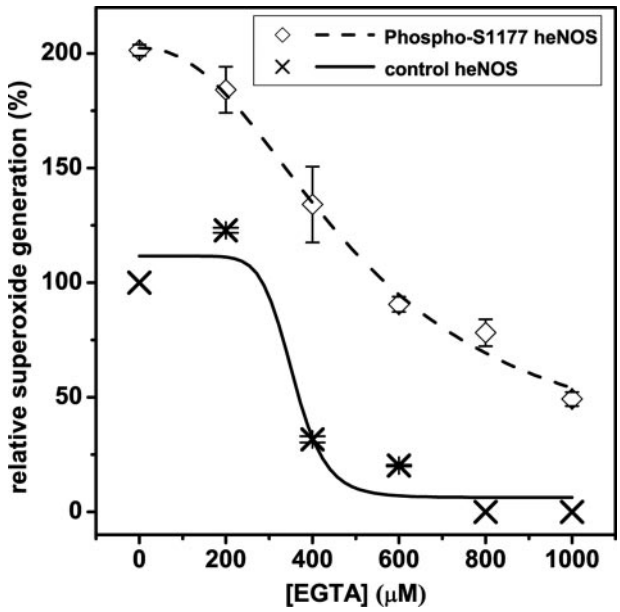

FIGURE 5. **EGTA inactivation of O_2^- generation by control heNOS and phospho-Ser-1177 heNOS.** O_2^- generation rates from control and phospho-Ser-1177 heNOS were determined by EPR spin-trapping with DEPMPO as described in Fig. 2. The effect of phosphorylation of heNOS on the EGTA inactivation of O_2^- generation was determined. 200 μM Ca^{2+} was included in the reaction. In control experiments, when EGTA was added to a final concentration of 800 μM, there is no measurable O_2^- generation, although with Akt phosphorylation, even with 1000 μM EGTA, still ~25% of the O_2^- generation remained. All data points show the relative magnitude of O_2^- generation compared with the maximal values measured from control heNOS and correspond to the mean ± S.E. from triplicate experiments. The line fitting of the experimental points for each curve was performed using a sigmoidal function.

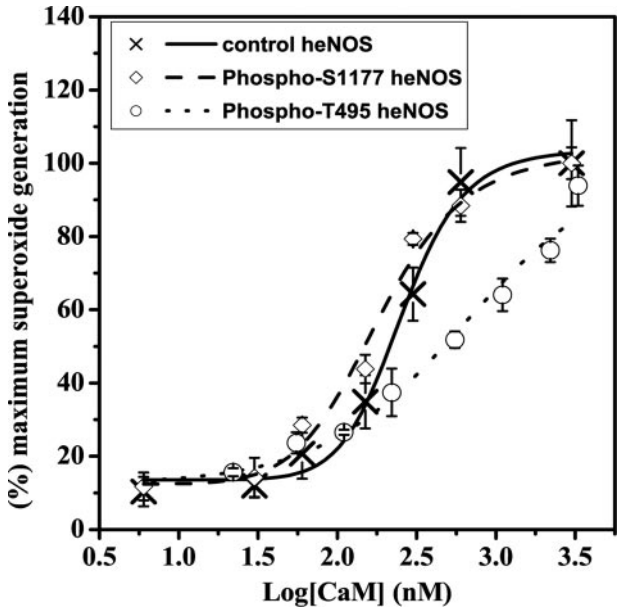

FIGURE 6. **CaM dependence of O_2^- generation from control, phospho-Ser-1177, and phospho-Thr-495 heNOS.** O_2^- generation rate from control, phospho- Ser-1177, and phospho-Thr-495 heNOS was determined from preparations of enzyme by EPR spin-trapping with DEPMPO as described in Fig. 2. The effect of phosphorylation of heNOS on the interaction with CaM under uncoupled (BH_4-free) conditions was determined. In the presence of 0.5 mM $CaCl_2$, CaM was added to the desired concentration as indicated. The concentration of CaM required for 50% maximal activity of O_2^- generation (EC_{50}) was determined from CaM dependence of heNOS O_2^- generation. The EC_{50} of control heNOS was 208 nM, the EC_{50} of phospho-Ser-1177 heNOS was 149 nM, and the EC_{50} of phospho-Thr-495 heNOS was 496 nM. Data were expressed as mean ± S.E., $n = 3$.

ity (Fig. 5). Even when EGTA was added to a final concentration of 1000 μM, the phosphorylated enzyme still retained ~25% of its maximal O_2^- generation capacity. Thus, it is clear that phosphorylation of heNOS at Ser-1177 increased resistance to EGTA inactivation of O_2^- generation.

CaM Dependence of Phosphorylation of heNOS on O_2^- Generation—The O_2^- generation rate of heNOS and phosphorylated heNOS at Ser-1177 was determined by EPR spin-trapping with DEPMPO, as a function of increasing concentrations of CaM. The calculated EC_{50} of control heNOS was 208 nM, and the calculated EC_{50} of phosphorylated heNOS at Ser-1177 was 149 nM (Fig. 6; Table 1); this result is consistent with the reported CaM dependence of NO production (21, 35). Furthermore, phosphorylation of heNOS by PKCα at Thr-495 greatly lowered its CaM binding affinity, increasing the calculated EC_{50} of Thr-495 phosphorylated heNOS to 496 nM (Fig. 6; Table 1).

Effects of Phosphorylation of heNOS on the Cav-P Inhibition of O_2^- Generation from Uncoupled heNOS—The association with caveolin is known to negatively regulate eNOS (36, 37). To investigate the effects of Cav-P on the O_2^- generation from control or phosphorylated heNOS, Cav-P was added to a final concentration of 400 μM. The percentage inhibition of O_2^- generation under each condition was used to determine how phosphorylation affects the association of heNOS with Cav-P. In control experiments using native enzyme, a 35.7% inhibition of O_2^- generation was produced by incubation with Cav-P. Phosphorylation in general produced an increase in Cav-P inhibition. When Ser-1177 was phosphorylated, Cav-P induced a 50.6% inhibition of O_2^- production, whereas with Thr-495 phosphorylation a 67.8% decrease of O_2^- was seen (Table 1).

Phosphorylation of eNOS Alters O_2^- Generation from Uncoupled eNOS in BAECs—To test how phosphorylation of eNOS affects the activity of uncoupled eNOS in endothelial cells, we treated BAECs with stimuli known to induce eNOS phosphorylation. We used confocal microscopy with DHE for the detection of O_2^- and phospho-specific eNOS antibodies to confirm the eNOS phosphorylation state in cells. Treatment of BAECs with VEGF and PMA is known to lead to the phosphorylation of eNOS on Ser-1179 and Thr-497 (equivalent to Ser-1177 and Thr-495 in the human eNOS), respectively (22). In control experiments, untreated BAECs, or untreated BAECs stimulated with VEGF, PMA, or CaI, there was no detectable DHE fluorescence signal. Thus, as expected, endothelial cells containing BH_4-repleted eNOS did not produce O_2^-, and phosphorylation of the enzyme did not lead to uncoupling.

To uncouple eNOS, BAECs were first treated with 5 mM 2,4-diamino-6-hydroxypyrimidine for 18 h to deplete BH_4 (32). In control BH_4-depleted cells, there was no detectable red HE fluorescence (Fig. 7*A*). Note, DAPI staining was used to counter stain the nuclei (*blue*). However, when the BH_4-depleted BAECs were treated with either CaI, commonly used to induce Ca^{2+} influx, or VEGF to induce Akt activation with phosphorylation of Ser-1179, strong red HE fluorescence was detected, and this stimulated O_2^- generation was completely inhibited by 1 mM L-NAME. This HE fluorescence was also completely quenched by the superoxide dismutase mimetic MnTBAP

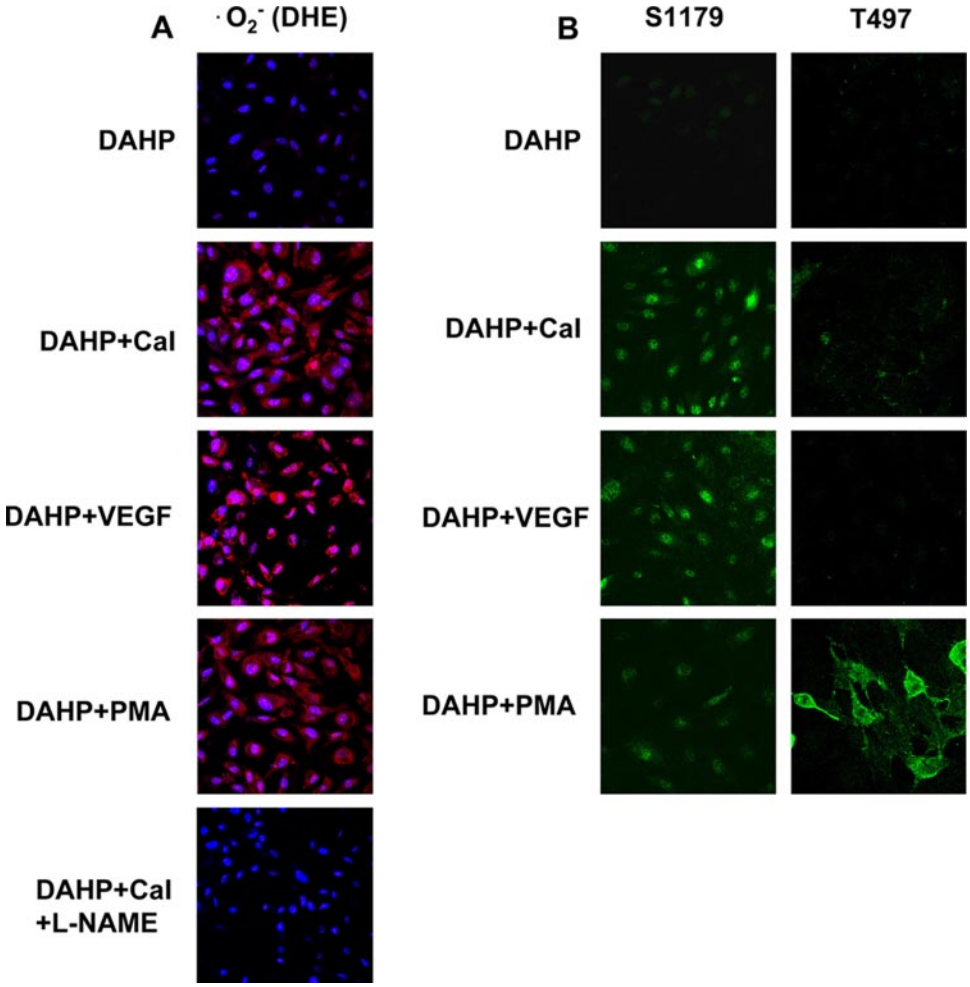

FIGURE 7. **Imaging of O_2^- generation and immunostaining in BAECs.** *A*, confocal microscopy measurements of O_2^- generation from uncoupled eNOS in endothelial cells. BH_4 depletion was achieved by incubation of BAECs with 5 mM 2,4-diamino-6-hydroxypyrimidine (*DAHP*) 18 h at 37 °C. The O_2^- generation was visualized from BH_4-depleted BAECs loaded with DHE that reacts to form HE, that exhibits red fluorescence. The *blue color* corresponds to the nuclei stained with DAPI. Measurable O_2^- fluorescence was seen only when the BH_4-depleted cells were treated with CaI, VEGF, or PMA, and this was inhibited by L-NAME. *B*, immunostaining using phosphorylation specific anti-eNOS antibodies in BH_4-depleted BAECs. The *left column* shows the results using the anti-phospho-Ser-1179 antibody. Ser-1179 phosphorylation was detected in BH_4-depleted BAECs when the cells were treated with CaI or VEGF but not with PMA. The *right column* shows the results using the anti-phospho-Thr-497 antibody, demonstrating that PMA treatment produced strong phosphorylation of Thr-497. These two immunostaining experiments were done in two sets of cells, both under the same conditions.

(manganese (III) tetrakis (4-benzoic acid) porphyrin), 1 mM, confirming that it was derived from O_2^- (data not shown). Treatment of BH_4-depleted BAECs with the PKC activator PMA, which increases intracellular Ca^{2+} and induces phosphorylation of Thr-497 (38), was performed, and these cells also exhibited red HE fluorescence similar to that induced by CaI. The phosphorylation of beNOS produced by each stimulus was determined by immunofluorescence microscopy using phospho-specific eNOS antibodies (Fig. 7*B*). Phosphorylation of uncoupled beNOS at Ser-1179 was seen when cells were treated with either VEGF or CaI, whereas treatment of BH_4-depleted cells with PMA led to the phosphorylation of eNOS mainly on Thr-497. Therefore, the formation of O_2^- from uncoupled beNOS in endothelial cells is stimulated by phosphorylation of the uncoupled enzyme at Ser-1179 or Thr-497 . Moreover, just as in our isolated enzyme experiments, phosphorylation of Thr-497 did not inhibit the formation of eNOS-derived O_2^-.

DISCUSSION

Nitric-oxide synthase requires BH_4 to produce NO from L-Arg in a reaction involving the NADPH-dependent formation of a heme-bound two-electron reduced molecular oxygen moiety. In the absence of BH_4, NOS is unable to timely donate the second electron, resulting in O_2^- release from the heme center, thus uncoupling NADPH oxidation from NO formation. The switch from NO to O_2^- production that is triggered by oxidative depletion of BH_4 has been implicated in the pathophysiology of numerous diseases (11, 39–43). Therefore, it is of critical importance to understand how the production of both of these eNOS-derived products is regulated.

Several sites have been identified in eNOS with the potential for phosphorylation and post-translational regulation, including Ser-1177, Thr-495, and serines 114, 615, and 633 (using the human amino acid numbering). However, prior work has shown that modifications of Ser-1177 and Thr-495 are of particular importance. It is commonly accepted that eNOS NO production is inhibited by phosphorylation at Thr-495 and enhanced by phosphorylation at Ser-1177 (20, 22, 44, 45). However, questions remain regarding the effect that phosphorylation of these two key residues has on the O_2^- production of the uncoupled enzyme. Therefore, in this work we have used EPR spin-trapping to determine how phosphorylation of recombinant human eNOS by native kinases affects the O_2^- production of the BH_4-free enzyme. We show that phosphorylation of Ser-1177 increased the rate of O_2^- generation by >50% in the presence of excess Ca^{2+}/CaM, whereas phosphorylation of Thr-495 had no effect under these conditions.

Phosphorylation of eNOS at Ser-1177 for human or Ser-1179 for bovine was first demonstrated to regulate its NO production in 1999 by Fulton *et al.* (18) and separately by Dimmeler *et al.* (19). It was shown that phosphorylation of this residue via the kinase Akt in cells leads to an increase in NOS-derived NO. Since then, isolated enzyme studies have shown that the S1177D eNOS mutant (mimicking the Ser-1177 phosphoryla-

ted eNOS) leads to an increase in the electron flow through the reductase domain, and it was hypothesized that this increase is the mechanism responsible for the phosphorylation-dependent increase in eNOS-derived NO (21).

In our current study, we directly demonstrate that under conditions where eNOS is uncoupled, phosphorylation of Ser-1177 increases the rate of O_2^- generation. With 80% phosphorylation of Ser-1177 we observe a 54% increase similar to that previously demonstrated for the phosphorylation-dependent increase in NO production. If one corrects for the incomplete phosphorylation, approximately a 68% increase in O_2^- generation would be expected with 100% phosphorylation of the enzyme. Moreover, we demonstrated in endothelial cells that this increase in O_2^- is also produced by Akt activation with phosphorylation of the critical serine. This increased O_2^- generation of phospho-Ser-1177 heNOS was inhibited by the addition of L-NAME, a NOS-specific inhibitor that blocks O_2^- formation by preventing electron transfer to the heme of the oxygenase domain. There has been a report that eNOS-dependent O_2^- generation from BAECs is not dependent upon Ser-1177 phosphorylation (46). Our results agree that phosphorylation is not required for the generation of O_2^- from eNOS. However, it is clear that Ser-1177 phosphorylation significantly increases O_2^- generation from eNOS and, perhaps more importantly, shifts the calcium requirement to much lower levels.

There are two potential mechanisms for O_2^- generation in eNOS, direct electron transfer from the FMN to molecular oxygen (commonly termed electron leakage) and electron transfer from the reductase domain to the oxygenase domain forming the ferrous heme, followed by oxygen binding and then regeneration of the ferric heme by the release of O_2^-. Because L-NAME blocked the observed increase in O_2^- in the phosopho-Ser-1177 eNOS, we conclude that Akt phosphorylation alters O_2^- production from the heme. The rate-limiting step for the generation of O_2^- from the heme is the transfer of electrons from the reductase domain to the oxygenase domain (47, 48), which in the global kinetic model of NOS activity proposed by Stuehr *et al.* (49) is the same rate-limiting step for NO production. Thus, it would be expected that any modification that alters eNOS NO production will similarly alter the activity of the uncoupled enzyme. Indeed, Ser-1177 phosphorylation increased the O_2^- production from the enzyme switching eNOS from Ca^{2+}-dependent to more Ca^{2+}-independent O_2^- generation, more like NOS-2. The EC_{50} for CaM activation of O_2^- production was also altered. These observations are in good agreement with reports measuring NO output from the S1177D eNOS and from an eNOS in which the C-terminal 27 amino acids (containing Ser-1177) were deleted (Δ27) (21, 50).

Both the C-terminal region of eNOS and an autoinhibitory region located in the FMN binding domain regulate the flow of electrons within the reductase domain, modulate CaM activation, and are thought to act in concert to regulate NOS function (51). Ser-1177 lies within the C-terminal region, and its phosphorylation is thought to regulate NO production from eNOS by altering the interaction between the C-terminal and autoinhibitory region (AR), releasing the AR-dependent inhibition. Along with the prior work using S1177D and Δ27, our data support this hypothesis. However, although Ser-1177 phosphorylation enhances the eNOS-CaM interaction, this phosphorylation event also would lead to an increase in the absolute rate of electron transfer from the reductase domain to the heme with increased flavin reduction rate, a hallmark of AR inhibition release (47).

Thr-495 lies within the CaM binding domain of eNOS, and the currently accepted dogma is that phosphorylation of eNOS at Thr-495 (human) or Thr-497 (bovine) inhibits NO production by interfering with CaM binding (27). However, more recent studies have questioned this. It has been shown that treatment of BAECs with okadaic acid and PMA, which increased Thr-497 phosphorylation, enhanced NO production compared with control (44). Moreover, although the T495A eNOS mutant, which mimics dephosphorylation, did increase NO production, mutagenesis of this residue to aspartic acid to mimic phosphorylation had no effect on eNOS NO activity (22). The dephosphorylation of Thr-495 has been linked to increasing eNOS-dependent O_2^- generation in endothelial cells via the inhibition of PKCα (52). Conversely it has been reported that PKCα overexpression activates eNOS and increases arterial blood flow *in vivo* (53), but it was hypothesized that this occurred due to an increase in Ser-1177 phosphorylation, not phosphorylation or dephosphorylation of Thr-495.

Our work demonstrated that phosphorylation of Thr-495 using PKCα did indeed greatly decrease CaM binding affinity; however, under conditions where CaM was saturating there was no effect on the maximal rate of O_2^- generation. Our cellular findings show strong heme-dependent O_2^- generation from BH_4-depleted BAECs even with the phosphorylation of Thr-495, clearly demonstrating that Thr-495 phosphorylation is not strictly an "off-switch." It has been shown that the cellular concentration of CaM is greater than 10 μM (54), which is higher than the saturating concentration of CaM used in our *in vitro* study. As such, although phosphorylation of Thr-495 does decrease CaM binding affinity for eNOS and thereby potentially leads to a decrease in eNOS activity, any potential negative regulation in cells would require alterations of other cellular factors that influence the eNOS-CaM interaction.

Previously it has been shown that the association of eNOS with caveolin inhibits eNOS activity (36, 37). Our results showed that the caveolin-dependent inhibition of eNOS O_2^- generation was enhanced by phosphorylation of eNOS, with the greatest inhibition seen when Thr-495 was phosphorylated. This indicates that phosphorylation of eNOS increases the association between eNOS and caveolin. As such, our *in vitro* data are consistent with the hypothesis that Thr-495 phosphorylation negatively regulates eNOS activity (13, 20, 22, 44, 52, 55, 56). Previous reports have indicated that phosphorylation of eNOS at Ser-1177 leads to a dissociation of eNOS and caveolin; however, this dissociation was dependent upon the induction of caveolin-dependent endocytosis (57, 58). We conclude that phosphorylation of heNOS at Thr-495 plays a role in the regulation of eNOS activity indirectly through the alteration of CaM binding and the association with caveolin. However, the precise *in vivo* regulation induced by Thr-495 phosphorylation will clearly be dependent upon processes that regulate local CaM and caveolin concentrations.

In the process of ischemia-reperfusion injury, the oxidative stress in tissues can lead to depletion of BH_4 (3, 4, 59). Recently

we have reported that hearts subjected to various durations of ischemia show a time-dependent decrease in BH_4 levels that trigger increased NOS-derived O_2^- production (60). Our current work demonstrates that with Akt-mediated phosphorylation, which would normally enhance eNOS-derived NO, increased eNOS-derived O_2^- production is also triggered from the uncoupled enzyme. Thus, when designing treatment strategies to ameliorate oxidative stress induced diseases by altering posttranslational modification of eNOS, one must consider that the activity of both coupled and uncoupled eNOS will be modified. For example, a strategy to enhance eNOS-derived NO by treatment with VEGF or other stimulus that induces Ser-1177 phosphorylation may exacerbate eNOS dysfunction in the post-ischemic heart. Moreover, although it was previously predicted that treatments to phosphorylate Thr-495 would decrease eNOS output, our data indicate that these would not necessarily decrease eNOS-derived O_2^- generation.

Our results demonstrate that phosphorylation can regulate O_2^- in addition to NO generation from eNOS. Peroxynitrite ($ONOO^-$) is formed by the diffusion-limited reaction of O_2^- and NO. Thus, $ONOO^-$ is a third potential eNOS-derived effector molecule regulated by the posttranslational modification of eNOS. Any modification that would partially uncouple eNOS, with generation of both O_2^- and NO, would lead to $ONOO^-$ generation. Additionally, any modification changing the flux of either O_2^- or NO from eNOS would alter the relative amount of $ONOO^-$ formed. $ONOO^-$ is known to be cytotoxic, functioning by both apoptotic and necrotic pathways (61). Additionally, $ONOO^-$ has been found to be a non-toxic signaling molecule, altering a number of cell signal transduction pathways (62). Thus, with partial BH_4 depletion, differential phosphorylation of eNOS could modulate $ONOO^-$ generation, leading to altered cell signaling or cell death.

In conclusion, PKCα-mediated phosphorylation of heNOS can decrease O_2^- production from the enzyme through alterations in its interactions with CaM and caveolin. Thus, Thr-495 phosphorylation indirectly regulates eNOS via modulation of protein-protein interactions. In contrast, Akt-mediated phosphorylation markedly enhances this O_2^- production directly by altering the kinetics of electron transfer within the enzyme. Additionally, this phosphorylation of Ser-1177 greatly increases O_2^- production at low levels of Ca^{2+} such that eNOS-dependent O_2^- generation becomes largely Ca^{2+}-independent. Thus, phosphorylation is of key importance in regulating the overall function, activation, and potentially the coupling, of eNOS, modulating both the production of NO and O_2^- from the enzyme.

Acknowledgment—We greatly appreciate the gift of pCWheNOS bacterial expression plasmid from Dr. Ortiz de Montellano (University of California San Francisco).

REFERENCES

1. Sessa, W. C. (2004) *J. Cell Sci.* **117,** 2427–2429
2. Kone, B. C., Kuncewicz, T., Zhang, W., and Yu, Z. Y. (2003) *Am. J. Physiol. Renal Physiol.* **285,** 178–190
3. Xia, Y., Tsai, A. L., Berka, V., and Zweier, J. L. (1998) *J. Biol. Chem.* **273,** 25804–25808
4. Vasquez-Vivar, J., Kalyanaraman, B., Martasek, P., Hogg, N., Masters, B. S., Karoui, H., Tordo, P., and Pritchard, K. A., Jr. (1998) *Proc. Natl. Acad. Sci. U. S. A.* **95,** 9220–9225
5. Muscoli, C., Cuzzocrea, S., Riley, D. P., Zweier, J. L., Thiemermann, C., Wang, Z. Q., and Salvemini, D. (2003) *Br. J. Pharmacol.* **140,** 445–460
6. Pou, S., Pou, W. S., Bredt, D. S., Snyder, S. H., and Rosen, G. M. (1992) *J. Biol. Chem.* **267,** 24173–24176
7. Xia, Y., Dawson, V. L., Dawson, T. M., Snyder, S. H., and Zweier, J. L. (1996) *Proc. Natl. Acad. Sci. U. S. A.* **93,** 6770–6774
8. Xia, Y., and Zweier, J. L. (1997) *Proc. Natl. Acad. Sci. U. S. A.* **94,** 6954–6958
9. Xia, Y., Roman, L. J., Masters, B. S., and Zweier, J. L. (1998) *J. Biol. Chem.* **273,** 22635–22639
10. Griffith, O. W., and Stuehr, D. J. (1995) *Annu. Rev. Physiol.* **57,** 707–736
11. Sun, J., Druhan, L. J., and Zweier, J. L. (2008) *Arch. Biochem. Biophys.* **471,** 126–133
12. Simoncini, T., Hafezi-Moghadam, A., Brazil, D. P., Ley, K., Chin, W. W., and Liao, J. K. (2000) *Nature* **407,** 538–541
13. Harris, M. B., Ju, H., Venema, V. J., Liang, H., Zou, R., Michell, B. J., Chen, Z.-P., Kemp, B. E., and Venema, R. C. (2001) *J. Biol. Chem.* **276,** 16587–16591
14. Igarashi, J., and Michel, T. (2001) *J. Biol. Chem.* **276,** 36281–36288
15. Morales-Ruiz, M., Lee, M. J., Zollner, S., Gratton, J. P., Scotland, R., Shiojima, I., Walsh, K., Hla, T., and Sessa, W. C. (2001) *J. Biol. Chem.* **276,** 19672–19677
16. Nagata, D., Takahashi, M., Sawai, K., Tagami, T., Usui, T., Shimatsu, A., Hirata, Y., and Naruse, M. (2006) *Hypertension* **48,** 165–171
17. Fulton, D., Gratton, J. P., and Sessa, W. C. (2001) *J. Pharmacol. Exp. Ther.* **299,** 818–824
18. Fulton, D., Gratton, J.-P., McCabe, T. J., Fontana, J., Fujiot, Y., Walsh, K., Franke, T. F., Papapetropoulos, A., and Sessa, W. C. (1999) *Nature* **399,** 597–601
19. Dimmeler, S., Fleming, I., Fisslthaler, B., Hermann, C., Busse, R., and Zeiher, A. M. (1999) *Nature* **399,** 601–605
20. Fleming, I., Fisslthaler, B., Dimmeler, S., Kemp, B. E., and Busse, R. (2001) *Circ. Res.* **88,** 68–75
21. McCabe, T. J., Fulton, D., Roman, L. J., and Sessa, W. C. (2000) *J. Biol. Chem.* **275,** 6123–6128
22. Lin, M. I., Fulton, D., Babbitt, R., Fleming, I., Busse, R., Pritchard, K. A., Jr., and Sessa, W. C. (2003) *J. Biol. Chem.* **278,** 44719–44726
23. Michell, B. J., Harris, M. B., Chen, Z. P., Ju, H., Venema, V. J., Blackstone, M. A., Huang, W., Venema, R. C., and Kemp, B. E. (2002) *J. Biol. Chem.* **277,** 42344–42351
24. Bucci, M., Gratton, J. P., Rudic, R. D., Acevedo, L., Roviezzo, F., Cirino, G., and Sessa, W. C. (2000) *Nat. Med.* **6,** 1362–1367
25. Gerber, N. C., and Ortiz de Montellano, P. R. (1995) *J. Biol. Chem.* **270,** 17791–17796
26. Rodriguez-Crespo, I., and Ortiz de Montellano, P. R. (1996) *Arch. Biochem. Biophys.* **336,** 151–156
27. Berka, V., Palmer, G., Chen, P. F., and Tsai, A. L. (1998) *Biochemistry* **37,** 6136–6144
28. Cardounel, A. J., Xia, Y., and Zweier, J. L. (2005) *J. Biol. Chem.* **280,** 7540–7549
29. Chen, Y. R., Chen, C. L., Yeh, A., Liu, X., and Zweier, J. L. (2006) *J. Biol. Chem.* **281,** 13159–13168
30. Bers, D. M., Patton, C. W., and Nuccitelli, R. (1994) *Methods Cell Biol.* **40,** 3–29
31. Patton, C., Thompson, S., and Epel, D. (2004) *Cell Calcium* **35,** 427–431
32. Delgado-Esteban, M., Almeida, A., and Medina, J. M. (2002) *J. Neurochem.* **82,** 1148–1159
33. Nathan, C., and Xie, Q. W. (1994) *Cell* **78,** 915–918
34. Gallis, B., Corthals, G. L., Goodlett, D. R., Ueba, H., Kim, F., Presnell, S. R., Figeys, D., Harrison, D. G., Berk, B. C., Aebersold, R., and Corson, M. A. (1999) *J. Biol. Chem.* **274,** 30101–30108
35. Michell, B. J., Griffiths, J. E., Mitchelhill, K. I., Rodriguez-Crespo, I., Tiganis, T., Bozinovski, S., de Montellano, P. R., Kemp, B. E., and Pearson, R. B. (1999) *Curr. Biol.* **9,** 845–848
36. Michel, J. B., Feron, O., Sacks, D., and Michel, T. (1997) *J. Biol. Chem.* **272,**

15583–15586
37. Ju, H., Zou, R., Venema, V. J., and Venema, R. C. (1997) *J. Biol. Chem.* **272,** 18522–18525
38. Andrews, D. A., Yang, L., and Low, P. S. (2002) *Blood* **100,** 3392–3399
39. Zweier, J. L., Flaherty, J. T., and Weisfeldt, M. L. (1987) *Proc. Natl. Acad. Sci. U. S. A.* **84,** 1404–1407
40. Zweier, J. L., Kuppusamy, P., and Lutty, G. A. (1988) *Proc. Natl. Acad. Sci. U. S. A.* **85,** 4046–4050
41. Zweier, J. L. (1988) *J. Biol. Chem.* **263,** 1353–1357
42. Zweier, J. L., Kuppusamy, P., Williams, R., Rayburn, B. K., Smith, D., Weisfeldt, M. L., and Flaherty, J. T. (1989) *J. Biol. Chem.* **264,** 18890–18895
43. Zweier, J. L. (1998) *Transplant. Proc.* **30,** 4228–4232
44. Michell, B. J., Chen, Z., Tiganis, T., Stapleton, D., Katsis, F., Power, D. A., Sim, A. T., and Kemp, B. E. (2001) *J. Biol. Chem.* **276,** 17625–17628
45. Greif, D. M., Kou, R., and Michel, T. (2002) *Biochemistry* **41,** 15845–15853
46. Whitsett, J., Martasek, P., Zhao, H., Schauer, D. W., Hatakeyama, K., Kalyanaraman, B., and Vasquez-Vivar, J. (2006) *Free Radic. Biol. Med.* **40,** 2056–2068
47. Haque, M. M., Panda, K., Tejero, J., Aulak, K. S., Fadlalla, M. A., Mustovich, A. T., and Stuehr, D. J. (2007) *Proc. Natl. Acad. Sci. U. S. A.* **104,** 9254–9259
48. Berka, V., Wu, G., Yeh, H. C., Palmer, G., and Tsai, A. L. (2004) *J. Biol. Chem.* **279,** 32243–32251
49. Stuehr, D. J., Santolini, J., Wang, Z. Q., Wei, C. C., and Adak, S. (2004) *J. Biol. Chem.* **279,** 36167–36170
50. Lane, P., and Gross, S. S. (2002) *J. Biol. Chem.* **277,** 19087–19094
51. Nishida, C. R., and Ortiz de Montellano, P. R. (1999) *J. Biol. Chem.* **274,** 14692–14698
52. Fleming, I., Mohamed, A., Galle, J., Turchanowa, L., Brandes, R. P., Fisslthaler, B., and Busse, R. (2005) *Cardiovasc. Res.* **65,** 897–906
53. Partovian, C., Zhuang, Z., Moodie, K., Lin, M., Ouchi, N., Sessa, W. C., Walsh, K., and Simons, M. (2005) *Circ. Res.* **97,** 482–487
54. Niki, I., Yokokura, H., Sudo, T., Kato, M., and Hidaka, H. (1996) *J. Biochem.* (*Tokyo*) **120,** 685–698
55. Chen, P. F., and Wu, K. K. (2000) *J. Biol. Chem.* **275,** 13155–13163
56. Chen, P. F., and Wu, K. K. (2003) *J. Biol. Chem.* **278,** 52392–52400
57. Maniatis, N. A., Brovkovych, V., Allen, S. E., John, T. A., Shajahan, A. N., Tiruppathi, C., Vogel, S. M., Skidgel, R. A., Malik, A. B., and Minshall, R. D. (2006) *Circ. Res.* **99,** 870–877
58. Lim, E. J., Smart, E. J., Toborek, M., and Hennig, B. (2007) *Am. J. Physiol. Heart Circ. Physiol.* **293,** 3340–3347
59. Xia, Y., Biondi, R., Liebgott, T., Paolocci, N., Cardounel, A., Ambrosio, G., and Zweier, J. L. (2004) *J. Am. Coll. Cardiol.* **43,** 294
60. Dumitrescu, C., Biondi, R., Xia, Y., Cardounel, A. J., Druhan, L. J., Ambrosio, G., and Zweier, J. L. (2007) *Proc. Natl. Acad. Sci. U. S. A.* **104,** 15081–15086
61. Szabo, C. (2003) *Toxicol. Lett.* **140–141,** 105–112
62. Pacher, P., Beckman, J. S., and Liaudet, L. (2007) *Physiol. Rev.* **87,** 315–424